Dual-beam optical trap based on microfabricated optical waveguides

M. M. van Leest, F. Bernal Arango[*)] and J. Caro

Kavli Institute of Nanoscience, Delft University of Technology, The Netherlands

We propose a novel design of the dual-beam trap for trapping and Raman identification of particles and biological objects in water. The device is based on Si_3N_4 waveguides launching counterpropagating beams into the fluidic channel of a lab-on-chip. For waveguides with a square cross section of 1 μm^2, a 5 μm gap between them and a 785 nm operation wavelength, we perform simulations of the beam profiles and the trapping forces acting on polystyrene beads (diameter 0.2-1.4 μm). The forces reach values up to 12 pN/Watt, indicating high suitability for particle trapping in a fluidic environment.

1. Introduction and approach

In bio-sensing there is a focus on the combination of photonics with lab-on-chip techniques [1]. In this field the miniaturization of optical tweezers by using waveguides, giving a new version of Ashkin's dual-beam trap [2] which avoids laser beams, is a challenge. Fibers [3,4] have been used to form such a trap, leading to prototypes integrated with a lab-on-chip. However, fibers traps are not suited for mass production, as required in areas such as in water-quality monitoring and medical diagnostics.

Here, we propose a novel design of the dual-beam trap for trapping of particles and biological objects in water, and study its properties from simulations. The device is based on microfabricated Si_3N_4 solid-core waveguides which launch counterpropagating beams into a fluidic channel. The waveguides are cladded by SiO_2. In the channel the concentrated optical field may induce the Raman fingerprint of the trapped object.

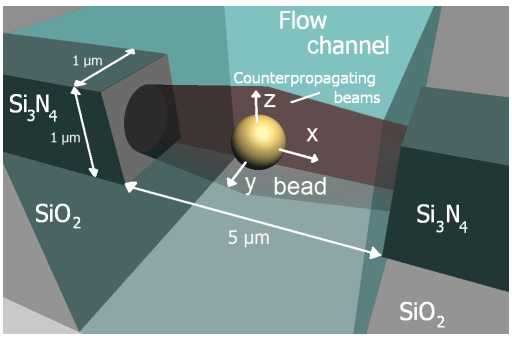

Fig. 1. Sketch of the dual-beam trap based on microfabricated Si_3N_4 waveguides.

We choose 1 μm^2 square cross-section waveguides, in easy reach of standard fabrication technology. The 5 µm gap between the waveguide facets equals the fluidic channel width. See Fig. 1, which also defines the axes of the system. This gap size is compatible with various biological objects, for instance certain bacteria. We use Si_3N_4 as waveguide material since it can operate at the near-visible and visible wavelengths used in Raman spectroscopy and for its compatibility with microfluidic technology. Further, Si_3N_4 and SiO_2 have good index contrast (n_{Si3N4}=1.9 versus n_{SiO2}=1.45). We establish the properties of the trap from finite-difference time-domain (FDTD) simulations of the beam properties and by calculating the trapping force acting on polystyrene beads. The simulations are carried out for the Raman excitation wavelength λ=785 nm, for which the waveguide can accommodate up to 8 modes per polarization direction.

[*)] present affiliation: FOM Institute AMOLF, Amsterdam, The Netherlands.

2. Characteristics of the single beam and the combined beams

Since the mode structure of these waveguides and the exiting beams cannot be obtained analytically, we perform simulations with the 3D FDTD method [5]. The excitation source is *y*-polarized, exciting modes with field components E_y and H_z. It delivers 0.5 W optical power to the waveguide. The fluidic medium is water (n_{H2O}=1.33).

Fig. 2 gives plots for the beam exiting a waveguide, simulated for a 4 μm source-facet distance. The red color in Fig. 2a represents the electric field intensity in the *xy*-plane, averaged over a time interval where the solution has converged to remove the intensity modulation in the water region. Figs. 2b and 2c show the averaged intensity profile on the *y*- and *x*-axis, respectively.

The most important feature in Fig. 2a is beam spreading, which is due to diffraction at the waveguide facet. For counterpropagating beams this leads to a non-zero scattering force, which drives a particle to the trap centre for an axial displacement [2]. The intensity pattern inside the waveguide shows a modulation on top of a maximum, seen more clearly in Fig. 2c. The modulation arises from interference of the wave sent by the source and the wave partially reflected at the facet. The maximum is part of a multimode interference (MMI) pattern [6]. This occurs as a result of excitation of several modes by the source, which presently is not tailored to selectively excite the lowest mode. For the transverse and the axial profile, a bell-shaped and a decaying curve are observed, respectively, which is as expected. The smaller maximum in the axial direction before the decay is the continuation of the MMI pattern formed inside the waveguide. Details of the transverse and axial curves depend on the source-facet distance, which influences the MMI pattern. However, the main characteristics needed for trapping, *viz.* the bell shape and the decay, are seen for each source position.

As a further step, we obtain for the complete dual-beam trap the averaged intensity distribution, without bead and with a 1 μm polystyrene bead at the point (0, 1, 0), again using a 4 μm source-facet distance. The sources oscillate in phase, each delivering 0.5 W of optical power. Fig. 3 shows the results for the *xy*-plane, without bead (a) and with bead (b). Contrary to Fig. 2a, averaging leaves intact the $\lambda_{H2O}/2$=295 nm periodicity in the water region, since interference now gives a standing wave pattern. The interfering beams yield an overall intensity distribution that will give a gradient force for radial and a scattering force for axial displacements. When comparing Figs. 3a and 3b, the

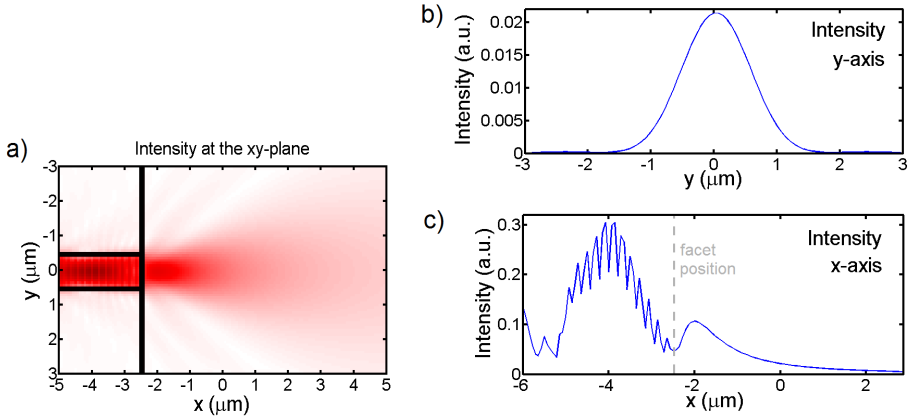

Fig. 2. Simulated intensity distribution of the electrical field in the *xy*-plane for the 1 μm^2 cross-section square waveguide (a), and transverse (b) and axial (c) intensity profile for this waveguide. In (a) the normalization is such that the full color scale is used.

disturbance of the field distribution by the bead is apparent. Owing to the higher index of the bead ($n_{polyst.}$=1.6) compared to that of water, it concentrates the electrical field inside its volume, also perturbing the field in its vicinity.

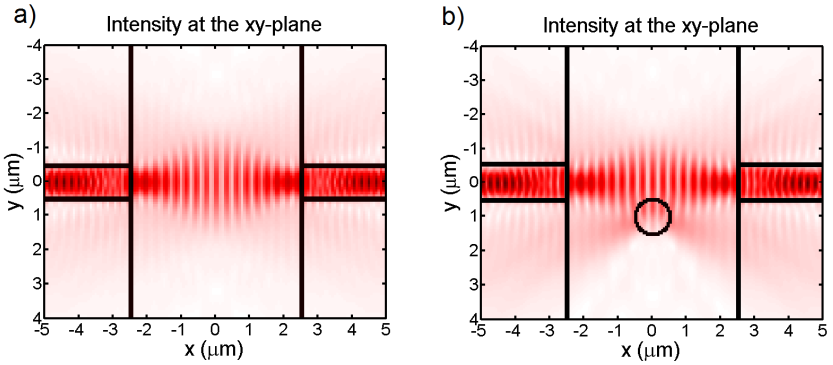

Fig. 3. Averaged intensity distribution in the *xy*-plane for the dual-beam trap based on 1 μm^2 cross-section square waveguides, without bead (a) and with a 1 μm diameter polystyrene bead centered at point (0, 1, 0) (b). The normalization is such that the full color scale is used.

4. Force characteristics of the dual-beam trap

We determine the trapping forces on the three axes from the simulated optical fields. Polystyrene beads of diameter 0.2, 0.5, 0.8, 1.0 and 1.4 μm serve as force probes. The force is evaluated by integrating the Maxwell stress tensor [7], using a cube of side $a = 2(r + \text{res})$ enclosing the bead (r=bead radius; res=1 μm/20 is the grid resolution).

In Fig. 4 we present the resulting curves, for the *x*- and *y*-direction (results for the *z*- and *y*-direction are the same, to within the accuracy for the grid resolution). For the *y*-direction the force is linear around the centre, *i.e.* it follows the usual Hookean law and defines a stable trapping point at the trap centre. With increasing distance, the force shows an extremum of which the |*x*|-position increases with increasing bead size. This bead-size dependence indicates operation outside the Rayleigh regime, consistent with the appreciable field disturbance by the particle shown Fig. 3b. The maximum trapping force is 12 pN/W (1.4 μm bead), in the *y*- and *z*-direction. The maximum trap stiffness thus is 0.03 pN/nm/W, a value very suitable for trapping.

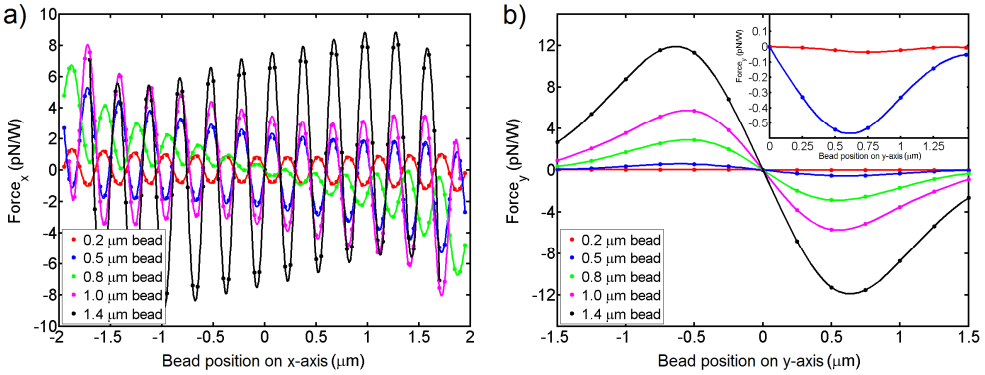

Fig. 4. Calculated forces in the *x*- and *y*-direction for several bead diameters (a, b). The inset in (b) is a blow up of the force curve for positive positions of the 0.2 and 0.5 μm diameter beads. The oscillatory curves in (a) are polynomial fits to the simulated points.

For the *x*-direction strong force oscillations are superimposed on a weak background. The oscillation period is 297 nm, consistent with the periodicity in Fig. 3. Thus, the oscillations relate to beam interference. We argue that in the gap region a 1D optical. lattice is formed. At x=0 the oscillatory curve for 0.2 and 0.8 μm has a negative slope, indicating a gradient force pushing beads to the intensity maximum. For 0.5 and 1.0 μm, on the contrary, the slope is positive, pushing the beads to an intensity minimum. This behavior, including its spatial oscillatory character, agrees completely with the results of Zemánek *et al.* [8], who theoretically study forces on wavelength-size polystyrene beads in a 1D optical lattice in water. These authors find that the oscillatory force depends periodically on the particle size, *i.e.* as a function of size the equilibrium position alternates between maxima and minima. Apparently, the two types of behavior we identify agree with the results in [8]. The behavior for the 1.4 μm bead is the same as for the 0.5 and 1.0 μm beads. The background, however, has a positive slope, contrary to the usual negative slope found for the other bead sizes. This sign reversal so far has not been properly analysed. The phase of the force oscillations in the *x*-direction depends on the relative phase of the beams, so that in a real device this dependence enables moving the particle in the *x*-direction by changing the relative phase.

6. Summary

In summary, we simulate a novel dual-beam optical trap based on Si_3N_4 waveguides, for (near-)visible wavelengths and compatible with microfluidic technology. The maximum force on 1.4 μm polystyrene beads is 12 pN/W, corresponding to a trap stiffness of 0.03 pN/nm/W, a value comparable to that of fiber-based traps. We envision that this dual-beam trap, when accommodated with a miniaturized Raman spectrometer, may fulfill requirements for on-line sensing of drinking water and medical diagnostics.

Acknowledgement

The authors gratefully acknowledge the financial support of Wetsus, the Dutch centre of excellence for sustainable water technology, and active involvement of participants of the Wetsus research theme ”Sensoring”. This work was also supported by the section Structural Optimization and Computational Mechanics of the Department of Precision and Microsystems Engineering of Delft University of Technology, by giving access to the Linux cluster hpc06.

References

[1] Xudong Fan, Ian M. White, Siyka I. Shopova, Hongying Zhu, Jonathan D. Suter and Yuze Sun, “Sensitive optical biosensors for unlabeled targets: A review”, Anal. Chim. Acta **620**, 8 (2008).

[2] Ashkin, “Acceleration and Trapping of Particles by Radiation Pressure”, Phys. Rev. Lett. **24**, 156 (1970).

[3] A. Constable *et al.*, “Demonstration of a fiber-optical light-force trap”, Opt. Lett. **18**, 1867 (1993).

[4] C. Jensen-McMullin *et al.*, “Demonstration of trapping, motion control, sensing and fluorescence detection of polystyrene beads in a multi-fiber optical trap," Opt. Express **13**, 2634 (2005).

[5] We use the package MEEP. See: Ardavan F. Oskooi *et al.*, “Meep: A flexible free-software package for electromagnetic simulations by the FDTD method”, Comput. Phys. Commun. **3**, 687 (2010).

[6] R. Ulrich and T. Kamiya, “Resolution of self-images in planar optical waveguides”, J. Opt. Soc. Am. **68**, 583 (1978).

[7] J. D. Jackson, Classical Electrodynamics, New York, Wiley, Ch. 6, pp. 258-262, 1998.

[8] P. Zemánek, A. Jonás and M. Liska, “Simplified description of optical forces acting on a nanoparticle in the Gaussian standing wave”, J. Opt. Soc. Am. A **19**, 1025 (2002).